International Journal of Thermophysics, Vol. 22, No. 4, 2001

Vapor-Phase Helmholtz Equation for HFC-227ea from Speed-of-Sound Measurements[1]

G. Benedetto,[2] R. M. Gavioso,[2] R. Spagnolo,[2] M. Grigiante,[3] and G. Scalabrin[3, 4]

This work presents measurements of the speed-of-sound in the vapor phase of 1,1,1,2,3,3,3-heptafluoropropane (HFC-227ea). The measurements were obtained in a stainless-steel spherical resonator with a volume of $\sim 900\ cm^3$ at temperatures between 260 and 380 K and at pressures up to 500 kPa. Ideal-gas heat capacities and acoustic virial coefficients are directly produced from the data. A Helmholtz equation of state of high accuracy is proposed, whose parameters are directly obtained from speed-of-sound data fitting. The ideal-gas heat capacity data are fit by a functions and used when fitting the Helmholtz equation for the vapor phase. From this equation of state other thermodynamic state function are derived. Due to the high accuracy of the equation, only very precise experimental data are suitable for the model validation and only density measurements have these requirements. A very high accuracy is reached in density prediction, showing the obtained Helmholtz equation to be very reliable. The deduced vapor densities are furthermore compared with those obtained from acoustic virial coefficients with the temperature dependences calculated from hard-core square-well potentials.

KEY WORDS: acoustic virial coefficient; Helmholtz energy equation of state; ideal gas heat capacity; speed-of-sound; vapor density; 1,1,1,2,3,3,3-heptafluoropropane (HFC-227ea).

1. INTRODUCTION

In the last few years new experimental techniques have resulted in high accuracy speed-of-sound measurements. These accurate acoustic data can

[1] Paper presented at the Fourteenth Symposium on Thermophysical Properties, June 25–30, 2000, Boulder, Colorado, U.S.A.

[2] Istituto Elettrotecnico Nazionale Galileo Ferraris, strada delle Cacce 91, I-10135 Torino, Italy.

[3] Dipartimento di Fisica Tecnica, Università di Padova, via Venezia 1, I-35131 Padova, Italy.

[4] To whom correspondence should be addressed. E-mail: gscala@unipd.it

0195-928X/01/0700-1073$19.50/0

be used to fit thermodynamic equations of state from which other thermodynamic properties can be calculated. This work presents new speed-of-sound measurements obtained in the vapor phase of 1,1,1,2,3,3,3-heptafluoropropane (HFC-227ea) and a simple and original method for converting these data into a Helmholtz energy equation. Contrary to the conventional methods adopted to reduce these kinds of measurements, the coefficients of the proposed equation have been fitted directly to speed-of-sound data, avoiding the use of either potential models or complex integration procedures generally utilized in conventional methods. The proposed equation has been validated with vapor phase density data, and the high accuracy achieved shows that this kind of procedure is capable of yielding reliable results well beyond the range of temperature and pressure in which the equation has been fitted.

2. APPARATUS, MATERIALS, AND PROCEDURES

The experimental apparatus consisted of a spherical resonator, placed in a temperature-controlled stirred fluid bath. A detailed description of the apparatus and the resonator has been given in a previous publication [1]. Temperatures were measured on ITS-90 using two capsule-type platinum resistance thermometers embedded in cylindrical extensions of the resonator poles. Pressures were measured to within an estimated uncertainty of 100 Pa using a capacitive absolute transducer calibrated against standard reference pressure balances in the range 0 to 500 kPa. The HFC-227ea sample was supplied by Solvay Fluor (D) with a stated minimum purity of 99.99 mole per cent. Before use, it was degassed by vacuum sublimation. No analysis or further purification was attempted.

Each isotherm included measurements of the speed of sound at several pressures. At each state point, the speed of sound was deduced from the measured resonance frequencies and calculated half-widths of the lowest three or four purely radial modes of the cavity. Experimental frequencies were corrected according to the model developed by Moldover [2] to account for thermal boundary layer losses, effects of coupling with shell motion, and the presence of the gas-inlet port. For the present measurements, the thermal boundary layer correction is the most important. This was calculated using thermal conductivity data measured by Liu [3]. All of the remaining corrections were very small, and they were included for the sake of completeness.

The thermodynamic and transport properties of HFC-227ea required for these corrections were obtained from the REFPROP database [4]. The speeds of sound determined from the individual modes were averaged together, then weighted by the statistical variance between the resonance

Table I. Mean Speed-of-Sound Values $\langle u \rangle$ of HCF-227ea Determined from N Radial Modes with Fractional Standard Deviations $\delta = [\langle u_{exp} \rangle - u_{fit}]/u_{fit}$ from Eq. (1) at Temperatures T and Pressures p

T (K)	p (kPa)	$\langle u \rangle$ (m·s^{-1})	N	$10^5\delta$	T (K)	p (kPa)	$\langle u \rangle$ (m·s^{-1})	N	$10^5\delta$
270.022	118.8	114.0606	4	3.3	280.022	174.2	114.5341	4	−8.6
	107.6	114.5427	4	−0.9		157.7	115.1879	4	−4.2
	96.14	115.0289	4	0.7		140.5	115.8699	4	0.1
	84.12	115.5300	4	2.1		122.7	116.5416	4	2.0
	72.13	116.0214	4	3.8		105.1	117.2028	4	1.7
	60.09	116.5073	4	5.4		87.19	117.8689	3	0.7
	48.08	116.9860	4	5.4		69.85	118.4977	3	0.9
	36.06	117.4602	4	3.9		52.31	119.1221	3	1.5
	23.96	117.9312	4	1.7		34.88	119.7346	3	0.1
	12.03	118.3890	4	−0.3		17.58	120.3333	3	−1.9
290.047	249.1	114.5902	4	−10.1	299.928	349.1	114.0709	4	−3.3
	225.4	115.4722	4	−4.9		315.5	115.2566	4	−0.1
	200.3	116.3819	4	−0.9		280.5	116.4607	4	1.6
	175.3	117.2686	4	2.5		245.5	117.6269	4	2.6
	150.3	118.1362	4	4.5		210.4	118.7624	4	3.4
	125.2	118.9878	4	4.5		175.4	119.8622	4	5.2
	98.65	119.8735	3	2.2		140.3	120.9363	4	5.5
	74.76	120.6505	3	1.2		105.2	121.9858	4	3.2
	49.81	121.4446	3	1.7		69.83	123.0182	3	1.9
	25.02	122.2205	3	0.3		35.00	124.0092	3	2.2
309.967	449.5	114.0298	4	5.5	329.948	500.2	119.2327	4	−2.2
	400.7	115.6454	4	2.8		450.6	120.5186	4	−5.3
	350.6	117.2359	4	3.1		400.5	121.7799	4	−6.2
	300.5	118.7679	4	3.0		350.5	123.0091	4	−6.0
	250.5	120.2462	4	2.8		300.3	124.2087	4	−5.6
	200.4	121.6744	4	3.1		249.5	125.3980	4	−5.7
	150.3	123.0559	4	4.1		198.7	126.5563	4	−4.5
	100.2	124.4024	4	1.6		149.7	127.6487	4	−2.5
	49.9	125.7113	3	2.3		100.1	128.7329	4	−2.9
						49.9	129.8064	3	−0.5
349.951	458.8	126.0383	4	−3.8	369.993	497.3	130.5475	4	9.7
	399.8	127.2190	4	−3.8		449.6	131.3376	4	5.2
	349.5	128.2068	4	−3.2		400.3	132.1396	4	4.9
	299.5	129.1707	4	−2.0		350.3	132.9494	4	0.8
	249.3	130.1283	4	−4.9		298.8	133.7663	4	1.6
	199.0	131.0663	4	−3.7		249.3	134.5422	4	1.9
	150.2	131.9634	4	−2.4		198.9	135.3249	4	2.1
	100.1	132.8719	4	−3.1		149.7	136.0811	4	1.4
	49.88	133.7691	3	−2.7		99.64	136.8424	2	0.1
						49.84	137.5926	2	−2.0

fits and the data. The resonance frequency measurements for HFC-227ea were taken along eight isotherms between 270 and 370 K and spanned pressures ranging from 12 to 500 kPa. Below 330 K the maximum pressure was 0.7 times the vapor pressure to avoid pre-condensation effects. The speed-of-sound values were obtained from the corrected resonance frequencies, together with the value of the resonator radius determined from a calibration with argon. In Table I we list mean values of the speed of sound for each of the 78 states investigated, together with fractional standard deviations and the number of resonant modes from which they were determined.

3. EXPERIMENTAL RESULTS

The speed-of-sound results have been analyzed in terms of the series expansion:

$$u^2(p, T) = (RT\gamma^o/M)[1 + (\beta_a/RT)\, p + (\gamma_a/RT)\, p^2 + (\delta_a/RT)\, p^3 + \cdots] \tag{1}$$

where β_a, γ_a and δ_a are the second, third and fourth acoustic virial coefficients respectively, which are functions of temperature only. In this equation, $R = 8.314471\ \mathrm{J \cdot mol^{-1} \cdot K^{-1}}$ is the universal gas constant [5], and $\gamma^o = c_p^o/c_v^o$ is the ratio of the isobaric to the isochoric ideal-gas heat capacity. Equation (1) was fitted to acoustic data on each isotherm by adjusting the first three or four acoustic virial coefficients (up to γ_a or δ_a), depending on the statistical significance of the fit. Table II shows the results of

Table II. Ideal-Gas Heat Capacities and Second and Third Acoustic Virial Coefficients of HFC-227ea Determined from Isotherm Fits. Uncertainties are one Standard Deviation

T (K)	c_p^o/R	β_a ($\mathrm{cm^3 \cdot mol^{-1}}$)	γ_a ($\mathrm{cm^3 \cdot mol^{-1} \cdot kPa^{-1}}$)
270.022	15.350 ± 0.007	-1415.9 ± 2.4	-0.614 ± 0.020
280.022	15.704 ± 0.005	-1292.6 ± 1.2	-0.476 ± 0.006
290.047	16.030 ± 0.008	-1191.8 ± 2.4	-0.298 ± 0.020
299.928	16.339 ± 0.010	-1102.5 ± 2.0	-0.190 ± 0.010
309.967	16.671 ± 0.013	-1018.9 ± 2.2	-0.137 ± 0.010
329.948	17.300 ± 0.007	-873.1 ± 1.1	-0.086 ± 0.004
349.951	17.820 ± 0.007	-752.6 ± 0.6	-0.070 ± 0.001
369.993	18.337 ± 0.012	-656.1 ± 1.0	-0.041 ± 0.002

these isotherm fits. The heat capacity values in Table II can be represented by:

$$c_p^0/R = 8.7303 - 1.250 \times 10^{-3}(T/\mathrm{K}) + 1.547 \times 10^{-4}(T/\mathrm{K})^2 - 2.19 \times 10^{-7}(T/\mathrm{K})^3 \quad (2)$$

with a standard deviation $\delta = 0.016R$. The ideal-gas heat capacity c_p^0 is shown in Fig. 1a and as deviations from Eq. (2), calculated as $\Delta c_p^0/c_p^0 = (c_{p_{\mathrm{exp}}}^0 - c_{p_{\mathrm{calc}}}^0)/c_{p_{\mathrm{calc}}}^0$, in Fig. 1b. To our knowledge there is only one previous determination of c_p^0 for HFC-227ea [6].

The deviations from our results, which are shown in the same Fig. 1b, lie between $0.025R$ and $-0.25R$ in the overlapping temperature range and diverge further at higher temperatures. All the isotherms were then combined to define a surface $u(p, T)$, whose deviations from a fitted correlation were a measure of the internal consistency among the isotherms. The correlation yielded estimates of the first three density virial coefficients, B, C, and D, from the analysis of the acoustic data and suitable parameterized expressions for the acoustic virial coefficients defined by a hard-core square-well (HCSW) approximation of the intermolecular potential [7]. Figure 2 displays measurements and the "square-well" fit to the second acoustic virial coefficient β_a as a function of temperature. The surface $u(p, T)$ was fitted with eight adjustable parameters, while Eq. (2) was used to represent the experimental $\gamma^o(T)$ values required to calculate the temperature dependence of the acoustic virial coefficients. The regression led to the parameters: $b_{0B} = 184.527\ \mathrm{cm}^3 \cdot \mathrm{mol}^{-1}$, $\varepsilon/k_B = 449.55$ K, $r_B = 1.318$, $b_{0C} = 383.717\ \mathrm{cm}^3 \cdot \mathrm{mol}^{-1}$, $\varepsilon/k_C = 780.09$ K, $r_C = 1.070$, $b_{0D} = 264.17\ \mathrm{cm}^3 \cdot \mathrm{mol}^{-1}$, and $\varepsilon/k_D = 175.704$ K with $r_D = 2$. Here, b_{0i}, ε/k_i, and r_i are the co-volume, the scaled well depth, and the ratio of the width of the well to that of the hard core for the second B, third C, and fourth D virial coefficients, respectively. Figure 3 displays a comparison of the estimated temperature dependence $B(T)$ from this work with that obtained from p–ρ–T measurements [8–10].

4. GAS DENSITY DETERMINATION FROM SPEED OF SOUND

4.1. Reduction Procedure

The problem of deriving accurate and simple procedures to yield thermodynamic models from speed-of-sound data has become common as consistent and accurate experimental speed-of-sound data have been obtained, in particular, for the new refrigerants. Referring to the gas phase, the conventional method estimates the gas density from a virial-type equation of

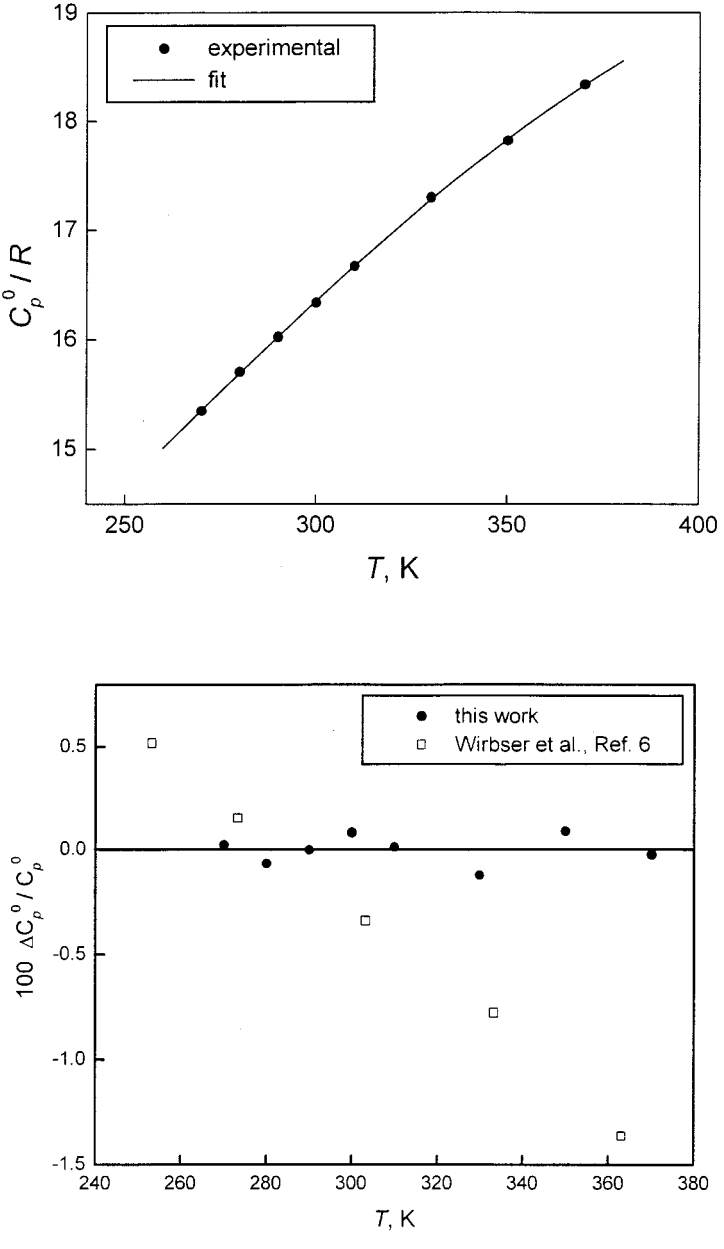

Fig. 1. (a) Measured ideal-gas heat capacities of HFC-227ea as a function of T. (b) Deviations of c_p^o from Eq. (2), calculated as $\Delta c_p^o / c_p^o = (c_{p_{\text{exp}}}^o - c_{p_{\text{calc}}}^o)/c_{p_{\text{calc}}}^o$. Measured values from Ref. 6 are also shown.

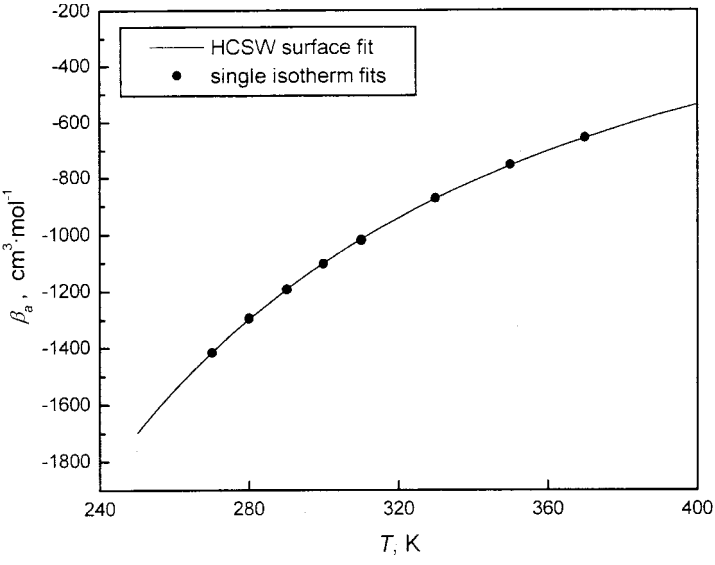

Fig. 2. Measurements and "square-well" fit to the second acoustic virial coefficient β_a as a function of temperature.

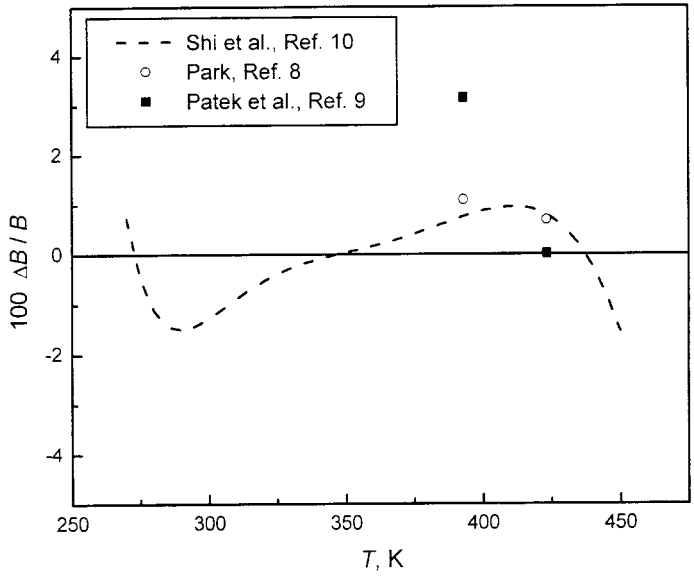

Fig. 3. Deviations of the measurements of the second density virial coefficient B of Ref. 8–10 from the model square well potential fitted with the parameters: $b_{0B} = 184.527\ \mathrm{cm}^3 \cdot \mathrm{mol}^{-1}$, $\varepsilon/k_B = 499.55$ K, and $r_B = 1.318$. The zero line refers to the present work.

state in which the temperature dependences of the first three density virial coefficients are calculated using the HCSW potential model [11, 12]. Among the presently available reduction methods, an original procedure has been recently proposed [13] consisting of the solution of the analytical relations between the density and the speed of sound and using a numerical integration procedure based on the predictor-corrector method. This method does not assume a specific type of equation of state, but it requires initial conditions usually referred to a particular isotherm close to the critical temperature.

In this work, a new and original approach of reducing speed-of-sound data is presented. The proposed procedure differs from previous ones as follows. First, a Helmholtz energy type equation is considered instead of the conventional virial equation. The structure of the selected equation comes from the optimization method proposed by Wagner and coworkers [14, 15], through which many modern high precision dedicated equations of state are obtained. This optimization procedure allows the selection from a so-called bank of $F_i(T, \rho)$ terms the combination which yields the smallest weighted least squares deviation after fitting the proposed terms to the experimental (P, ρ, T) values. The final form consists of an eight-term Helmholtz equation which conforms to the best result that can be obtained with this optimization method. Then, the parameters of the optimized equation are fitted directly to speed-of-sound data following a standard nonlinear fitting procedure. The values of the coefficients are estimated minimizing the weighted sum of squares of the calculated speed-of-sound data and the experimental values. In this way, contrary to the cited integration procedure, no initial conditions have to be specified and complex numerical computation methods can be avoided.

The Helmholtz energy equation is expressed in the following dimensionless form:

$$\phi(\tau, \delta) = \frac{A_m}{RT} = \phi^o(\tau, \delta) + \phi^R(\tau, \delta) \tag{6}$$

where A_m is the molar free energy, R is the universal gas constant, $\tau = T_c/T$ is the inverse reduced temperature, and $\delta = \rho/\rho_c$ is the reduced density. $T_c = 375.95$ K, and $\rho_c = 580.0\ \mathrm{kg \cdot m^{-3}}$ are the critical parameters of HFC-227ea [16]. The dimensionless form ϕ of Eq. (6) is split into an ideal part ϕ^o, which approximates the ideal behavior of the fluid, and a residual part ϕ^R which takes into account the real behavior of the fluid.

From the ideal gas heat capacity c_p^0, Eq. (5), the dimensionless ideal part ϕ^o can be expressed as:

$$\phi^o = \frac{A^o}{RT}$$

$$= \frac{1}{RT}\left\{\int_{T_0}^{T} c_p^o\, dT + h_0^o - RT - T\int_{T_0}^{T} \frac{c_p^o - R}{T}\, dT - RT[\ln(\rho/\rho_0)] - Ts_0^o\right\} \tag{6a}$$

where h_0^o and s_0^o are the enthalpy and entropy values of the ideal gas in a reference state. From the molar free energy equation expressed by Eq. (6), the speed of sound u is deduced from the following relation:

$$\frac{u^2(\tau, \delta)}{RT} = 1 + 2\delta\phi_\delta^R + \delta^2\phi_{\delta\delta}^R + \frac{(1 + \delta\phi_\delta^R - \delta\tau\phi_{\delta\tau}^R)^2}{c_v/R} \tag{7}$$

where ϕ_δ^R and $\phi_{\delta\delta}^R$ are the first and second derivatives of the residual part ϕ^R with respect to δ, while $\phi_{\delta\tau}^R$ is the cross-derivative of the residual part ϕ^R with respect to δ and τ. c_v is the isochoric heat capacity, which is related to the fundamental Eq. (6) by the relation:

$$\frac{c_v(\tau, \delta)}{R} = -\tau^2(\phi_{\tau\tau}^o + \phi_{\tau\tau}^R) \tag{8}$$

where $\phi_{\tau\tau}^o$ and $\phi_{\tau\tau}^R$ are the second derivatives, with respect to τ, of the ideal part ϕ^o and of the residual part ϕ^R, respectively.

In this work, the c_p^o function is obtained from the same speed-of-sound measurements, as shown in the preceding, and enables the derivative $\phi_{\tau\tau}^o$, required to calculate the c_v value, Eq. (8), to be determined directly from the known ideal gas relation:

$$c_p^o - c_v^o = R \tag{9}$$

All the derivatives are easily calculated from the following form of the residual part ϕ^R:

$$\phi^R(\tau, \delta) = \sum_{i=1}^{8} a_i \tau^{t_i} \delta^{d_i} \tag{10}$$

The main difference of the equation form with respect to a classical virial equation is the independence of the coefficients a_i, t_i, and d_i from temperature; besides, these coefficients are directly obtained fitting the speed-of-sound data without considering any potential energy model. The proposed procedure does not require the solution of a strict algorithm,

Table III. Coefficients for the Residual Part ϕ^r Regressed from Speed-of-Sound Data

n	a_n	t_n	d_n
1	2.5506366×10^{-1}	−0.5	2.0
2	$-5.8366183 \times 10^{-1}$	0.0	1.0
3	$1.86043256 \times 10^{-1}$	0.0	3.0
4	$-7.028444564 \times 10^{-3}$	0.0	6.0
5	$-2.586155308 \times 10^{-2}$	1.5	6.0
6	$3.519227878 \times 10^{0}$	1.5	1.0
7	$-4.1765737419 \times 10^{0}$	2.0	1.0
8	$-1.424392239 \times 10^{-3}$	2.0	2.0

avoiding the specific initial conditions proposed by Trusler [17]. Using a classical nonlinear regression procedure, the coefficients for the residual part ϕ^R are reported in Table III.

4.2. Model Validation

The obtained Helmholtz free energy equation has been validated with vapor phase density results comparing the calculated values with available experimental density data [10]. The results are expressed in terms of AAD% as shown in Figs. 4 to 7. The available density data cover the ranges $0.81 \leqslant T_r \leqslant 1.0$ and $0.033 \leqslant P_r \leqslant 0.74$, which differ significantly from

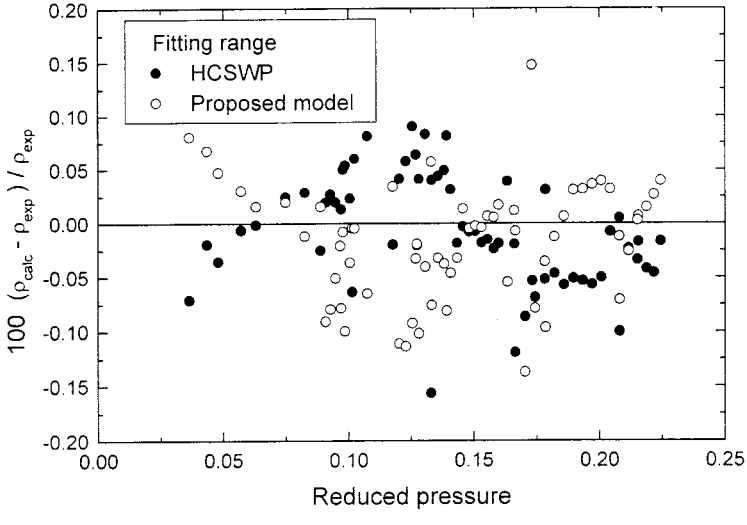

Fig. 4. Density validation of the Helmholtz free energy Eq. (6) as function of pressure and inside the fitting range.

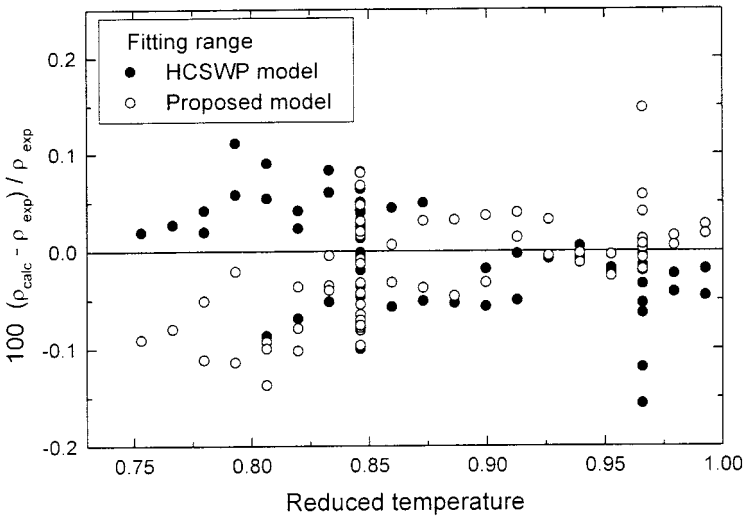

Fig. 5. Density validation of the Helmholtz free energy Eq. (6) as function of temperature and inside the fitting range.

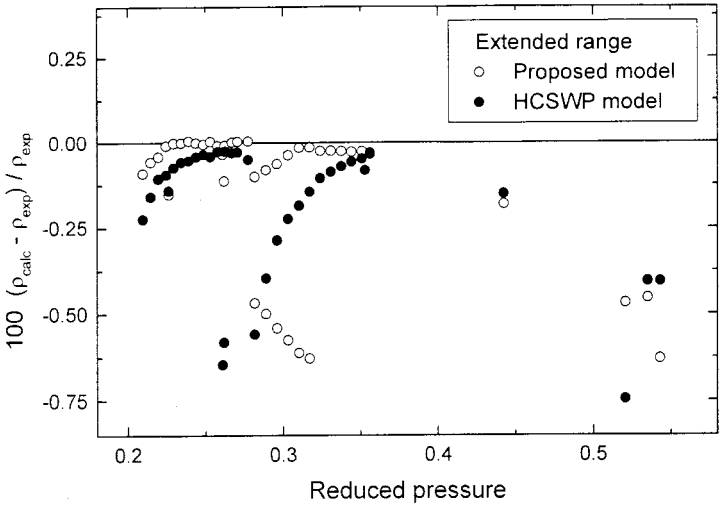

Fig. 6. Density validation of the Helmholtz free energy Eq. (6) as function of pressure and outside the fitting range.

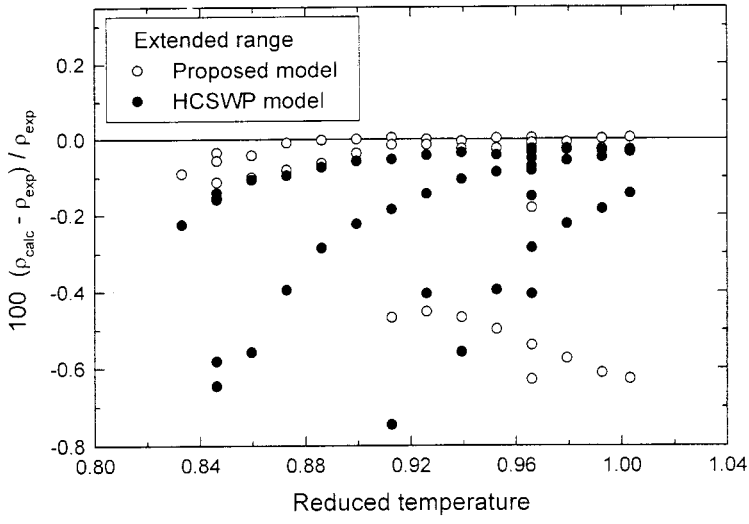

Fig. 7. Density validation of the Helmholtz free energy Eq. (6) as function of temperature and outside the fitting range.

the speed-of-sound measurement range, i.e., $0.72 \leqslant T_r \leqslant 0.98$ and $0.004 \leqslant P_r \leqslant 0.167$, on which the parameters have been based.

The accuracy of the proposed model in density prediction shows an AAD% of 0.00426, while the corresponding value of the HCSW model is 0.00428. The selected pressure range, outside the fitting range, in which the density data have been assumed was $0.226 \leqslant P_r \leqslant 0.542$. In this range the AAD% of the present model is 0.148 and that of the HCSW model is 0.182. A total of 65 points was inside the fitting range, and 55 were outside the range.

The thermodynamic virial coefficients are often considered because they can yield information on thermal properties in the gas phase. However, they are normally derived only from density or speed-of-sound experimental data, because of the higher accuracy of these data. Taking into account the virial coefficients definition and a Helmholtz energy type equation of state, we have

$$B(T) = \lim_{\rho \to 0} \left(\frac{\partial (p/\rho RT)}{\partial \rho} \right)_T \qquad \text{and} \qquad B(\tau)\, \rho_c = \lim_{\delta \to 0} \phi_\delta^R(\tau, \delta) \tag{11}$$

$$C(T) = \frac{1}{2} \lim_{\rho \to 0} \left(\frac{\partial^2 (p/\rho RT)}{\partial \rho^2} \right)_T \qquad \text{and} \qquad C(\tau)\, \rho_c^2 = \lim_{\delta \to 0} \phi_{\delta\delta}^R(\tau, \delta) \tag{12}$$

and similar expressions hold for the higher order coefficients $D(T)$, $E(T)$, etc. A Helmholtz equation can then be always transformed into a virial-like analytical form:

$$\frac{p}{\rho RT} = 1 + B(T)\,\rho + C(T)\,\rho^2 + D(T)\,\rho^3 + \cdots \tag{13}$$

where the coefficients are given by expressions derived from the $\phi^R(\tau, \delta)$ equation. For the present case, one gets from Eq. (10):

$$B(T) = [a_2 + a_6(T_c/T)^{1.5} + a_7(T_c/T)^2]/\rho_c \tag{14}$$

$$C(T) = \{2[a_1(T_c/T)^{-0.5} + a_8(T_c/T)^2]\}/\rho_c^2 \tag{15}$$

$$D(T) = 3a_3/\rho_c^3 \tag{16}$$

$$E(T),\ F(T) = 0 \tag{17}$$

$$G(T) = \{6[a_4 + a_5(T/T_c)^{1.5}]\}/\rho_c^6 \tag{18}$$

Since equations of state provide solutions for different properties, an equation that represents experimental speed-of-sound and $P\rho T$ data within their experimental uncertainty has to represent virial coefficients within their uncertainty as well. Unfortunately, the comparison between virial coefficients generated by use of different techniques is not completely consistent. For instance, the second and third virial coefficients values can be generated by forcing Eq. (13), truncated at the third term, to represent $P\rho T$ vapor data, and the obtained values correlated as temperature functions. It is not likely that the first two virial coefficients obtained from our complete Eq. (13) would be consistent with those obtained from the truncated equation used to represent density data.

Alternatively, the second ordinary virial coefficient can also be determined from speed-of-sound data through numerical integration of the second acoustical virial coefficient, provided initial conditions near the lowest isotherm are given. Also, ordinary virial coefficients of different order can be derived by assumption of an explicit functional form for the intermolecular potential [18].

For the second and third virial coefficients of R227ea, a few correlations and single values obtained from $P\rho T$ and speed-of-sound vapor data can be found in the literature. In Figs. 8 and 9 comparisons are made of the second and third virial coefficients as represented by the proposed equation of state, Eqs. (14) and (15), by our HCSW model and by Refs. 9 and 19. Among available literature sources only the HCSW correlation for

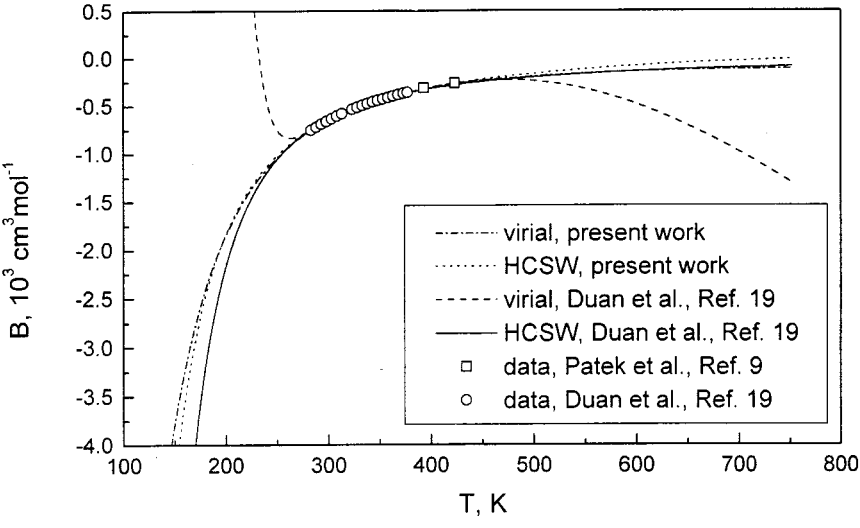

Fig. 8. Second thermodynamic virial coefficient B as function of temperature represented by the Helmholtz energy model, Eq. (14), and the HCSW model from the present work and from literature correlations and values.

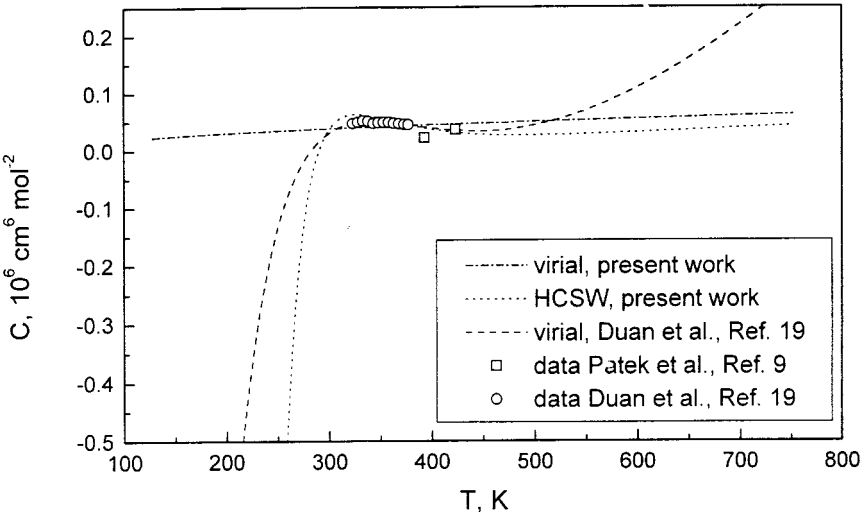

Fig. 9. Third thermodynamic virial coefficient C as function of temperature represented by the Helmholtz energy model, Eq. (15), and the HCSW model from the present work and from literature correlations and values.

$B(T)$ of Duan et al. [19] was determined from speed-of-sound data. It can be observed that correlations for virial coefficients derived by alternative techniques show significantly different behaviors.

Over the range of available experimental data the virial coefficients analytically derived from our equation of state are in satisfactory agreement with those obtained through different procedures. This was not surprising considering the high accuracy of the Helmholtz energy equation in representing density data. Outside the regression range, and even more outside the validation range, the virial coefficient functions can only be considered qualitative.

The B coefficient from our virial and HCSW functions, as well as the HCSW one reported by Duan et al. [19], give qualitatively correct plots, while the B coefficient obtained from density values by Duan et al. shows significant deviations outside the 250 to 450 K temperature range. All the correlations satisfactorily fit the data inside the experimental range.

As to the third virial coefficient C, our virial function shows a wrong trend though maintaining good quantitative agreement with the results of other researchers. Our HCSW function and the virial one from Duan et al. differ macroscopically, in particular, at low temperatures. The trend of the HCSW function is qualitatively correct, but unfortunately it is not possible to verify if the function is also quantitatively accurate.

5. CONCLUSIONS

In this work new speed-of-sound measurements were performed for 1,1,1,2,3,3,3-heptafluoropropane (HFC-227ea) in the vapor phase. The measurements span the temperature range from 270 to 370 K at pressures up to 500 kPa. Ideal-gas heat capacities and acoustic virial coefficients are deduced directly from the results.

A new procedure is proposed which determines the coefficients of an optimized Helmholtz energy equation form directly fitting the experimental speed-of-sound values. This method compares favorably with other conventional methods and provides a high accuracy equation specific for the vapor phase. The density values calculated from this equation are compared with existing experimental data in similar T_r and P_r ranges and also outside the fitting ranges. Inside the fitting range the error deviation is within $\pm 0.015\%$, while outside it reaches $\pm 0.7\%$.

An analysis of the virial coefficients behavior shows that the second coefficient B is well represented by both the proposed and the HCSW models, while the third coefficient C from the proposed model shows a wrong trend. Nevertheless, the virial coefficients obtained in this work give a good representation of the results of the available data.

Due to the low pressure range considered, the proposed structure of the equation is likely to fit directly speed-of-sound data in similar pressure ranges with similar precision for all the fluids belonging to the HCFC and HFC families. This leads to the conclusion that the Helmholtz equation can be a valid alternative to other approaches based on the use of classical virial and potential energy model equations.

REFERENCES

1. G. Benedetto, R. M. Gavioso, and R. Spagnolo, *La Rivista del Nuovo Cimento* **22**:1 (1999).
2. M. R. Moldover, J. B. Mehl, and M. Greenspan, *J. Acoust. Soc. Am.* **79**:253 (1986).
3. X. Liu, L. Shi, Y. Duan, L. Han, and M. Zhu, *J. Chem. Eng. Data* **44**:882 (1999).
4. M. Huber, J. Gallagher, M. McLinden, and G. Morrison, NIST Database 23 (REFPROP), Version 5.12 (National Institute of Standards and Technology, Gaithersburg, Maryland, 1996).
5. M. R. Moldover, J. P. M. Trusler, T. J. Edwards, J. B. Mehl, and R. S. Davis, *Phys. Rev. Lett.* **60**:249 (1988).
6. H. Wirbser, G. Brauning, J. Gurtner, and G. Ernst, *J. Chem. Thermodyn.* **24**:761 (1992).
7. K. A. Gillis and M. R. Moldover, *Int. J. Thermophys.* **17**:1305 (1997).
8. Y. J. Park, Thesis (Universität Karlsruhe, 1993).
9. J. Pátek, J. Klomfar, J. Prazák, and O. Šifner, *J. Chem. Thermodyn.* **30**:1159 (1998).
10. L. Shi, Y. Duan, M. Zhu, L. Han, and X. Lei, *J. Chem. Eng. Data* **44**:1402 (1999).
11. K. A. Gillis, *Int. J. Thermophys.* **18**:73 (1997).
12. A. Yokozeki, H. Sato, and K. Watanabe, *Int. J. Thermophys.* **19**:89 (1998).
13. A. F. Estrada-Alexanders and J. P. M. Trusler, *J. Chem. Thermodyn.* **29**:991 (1997).
14. R. Schmidt and W. Wagner, *Fluid Phase Equil.* **19**:175 (1985).
15. U. Setzmann and W. Wagner, *Int. J. Thermophys.* **10**:1103 (1989).
16. D. R. Defibaugh and M. R. Moldover, *J. Chem. Eng. Data* **42**:650 (1997).
17. A. F. Estrada-Alexanders, J. P. M. Trusler, and M. P. Zarari, *Int. J. Thermophys.* **16**:663 (1995).
18. A. R. H. Goodwin and M. R. Moldover, *J. Chem. Phys.* **93**:2741 (1990).
19. Y. Y. Duan, L. Shi, M. S. Zhu, L. Z. Han, and C. Zhang, submitted to *Int. J. Thermophys.* (2000).